Original Article | Gastrointestinal Imaging

eISSN 2005-8330
https://doi.org/10.3348/kjr.2023.0368
Korean J Radiol 2023;24(10):983-995

Korean Journal of Radiology
KJR

Comparison Between Contrast-Enhanced Computed Tomography and Contrast-Enhanced Magnetic Resonance Imaging With Magnetic Resonance Cholangiopancreatography for Resectability Assessment in Extrahepatic Cholangiocarcinoma

Jeongin Yoo[1], Jeong Min Lee[1,2,3], Hyo-Jin Kang[1,2], Jae Seok Bae[1,2], Sun Kyung Jeon[1], Jeong Hee Yoon[1,2]

[1]Department of Radiology, Seoul National University Hospital, Seoul, Republic of Korea
[2]Department of Radiology, Seoul National University College of Medicine, Seoul, Republic of Korea
[3]Institute of Radiation Medicine, Seoul National University Medical Research Center, Seoul, Republic of Korea

Objective: To compare the diagnostic performance and interobserver agreement between contrast-enhanced computed tomography (CECT) and contrast-enhanced magnetic resonance imaging (CE-MRI) with magnetic resonance cholangiopancreatography (MRCP) for evaluating the resectability in patients with extrahepatic cholangiocarcinoma (eCCA).

Materials and Methods: This retrospective study included treatment-naïve patients with pathologically confirmed eCCA, who underwent both CECT and CE-MRI with MRCP using extracellular contrast media between January 2015 and December 2020. Among the 214 patients (146 males; mean age ± standard deviation, 68 ± 9 years) included, 121 (56.5%) had perihilar cholangiocarcinoma. R0 resection was achieved in 108 of the 153 (70.6%) patients who underwent curative-intent surgery. Four fellowship-trained radiologists independently reviewed the findings of both CECT and CE-MRI with MRCP to assess the local tumor extent and distant metastasis for determining resectability. The pooled area under the receiver operating characteristic curve (AUC), sensitivity, and specificity of CECT and CE-MRI with MRCP were compared using clinical, surgical, and pathological findings as reference standards. The interobserver agreement of resectability was evaluated using Fleiss kappa (κ).

Results: No significant differences were observed between CECT and CE-MRI with MRCP in the pooled AUC (0.753 vs. 0.767), sensitivity (84.7% [366/432] vs. 90.3% [390/432]), and specificity (52.6% [223/424] vs. 51.4% [218/424]) (P > 0.05 for all). The AUC for determining resectability was higher when CECT and CE-MRI with MRCP were reviewed together than when CECT was reviewed alone in patients with discrepancies between the imaging modalities or with indeterminate resectability (0.798 [0.754–0.841] vs. 0.753 [0.697–0.808], P = 0.014). The interobserver agreement for overall resectability was fair for both CECT (κ = 0.323) and CE-MRI with MRCP (κ = 0.320), without a significant difference (P = 0.884).

Conclusion: CECT and CE-MRI with MRCP showed no significant differences in the diagnostic performance and interobserver agreement in determining the resectability in patients with eCCA.

Keywords: Extrahepatic cholangiocarcinoma; Klatskin tumor; Multidetector computed tomography; Magnetic resonance imaging; Magnetic resonance cholangiopancreatography

INTRODUCTION

Cholangiocarcinoma (CCA) is the second most common hepatobiliary malignancy after hepatocellular carcinoma [1], accounting for 10%–15% of all primary liver cancers [2]. It is subclassified as intrahepatic CCA and extrahepatic

Received: April 22, 2023 **Revised:** July 19, 2023 **Accepted:** July 31, 2023
Corresponding author: Jeong Hee Yoon, MD, Department of Radiology, Seoul National University Hospital, Seoul National University College of Medicine, 101 Daehak-ro, Jongno-gu, Seoul 03080, Republic of Korea
• E-mail: cinamon1@snu.ac.kr

CCA (eCCA), with frequencies of 10%–20% and 80%–90%, respectively; the latter is further subdivided into perihilar CCA and distal CCA [2]. Currently, surgical resection is the only curative treatment option for the prolonged survival of patients with eCCA, and an accurate preoperative imaging assessment is critical to avoid futile surgery and achieve R0 resection [3].

Contrast-enhanced computed tomography (CECT) and contrast-enhanced magnetic resonance imaging (CE-MRI) are the most commonly used imaging modalities for preoperative tumor staging and resectability assessment in patients with eCCA. CECT assesses the extent of eCCA by revealing distant metastasis and its relationship with the adjacent vessels, such as the hepatic artery and portal vein [1,4]. Therefore, CECT is considered the initial standard imaging modality for patients with suspected eCCA [1,5]. CE-MRI with magnetic resonance cholangiopancreatography (MRCP) provides detailed information regarding the bile duct anatomy and longitudinal extent of the eCCA. A recent guideline issued by the Korean Society of Abdominal Radiology (KSAR) study group for eCCA [6] recommends using CECT and/or CE-MRI with MRCP to evaluate the resectability of eCCA. However, only a few studies [7-9] have compared the diagnostic performance between CE-MRI with MRCP and CECT for assessing eCCA resectability. Therefore, this study aimed to compare the diagnostic performance and interobserver agreement between CECT and CE-MRI with MRCP for evaluating the resectability in patients with eCCA.

MATERIALS AND METHODS

This retrospective study was approved by Seoul National University Hospital Institutional Review Board, and the requirement for informed consent was waived (IRB No. 1908-134-1057).

Study Population

A search of the database at Seoul National University Hospital yielded 799 patients with pathologically confirmed biliary tract cancers between January 2015 and December 2020 (Fig. 1). The inclusion criteria were age > 18 years and both CECT and CE-MRI with MRCP performed to evaluate the resectability of histologically confirmed eCCA. Among the 587 patients who met the inclusion criteria, 373 were excluded for the following reasons: 1) computed tomography (CT)/magnetic resonance imaging (MRI) with biliary stent insertion (n = 117); 2) gadoxetic acid-enhanced MRI (n = 106); 3) single-phase CT (n = 77); 4) no reference standard for resectability (n = 48); 5) interval > 6 weeks between CECT and CE-MRI (n = 17); 6) neoadjuvant therapy for eCCA (n = 6); and 7) poor image quality (n = 2). Finally, this study included 214 patients (146 males; mean age ± standard deviation, 68 ± 9 years).

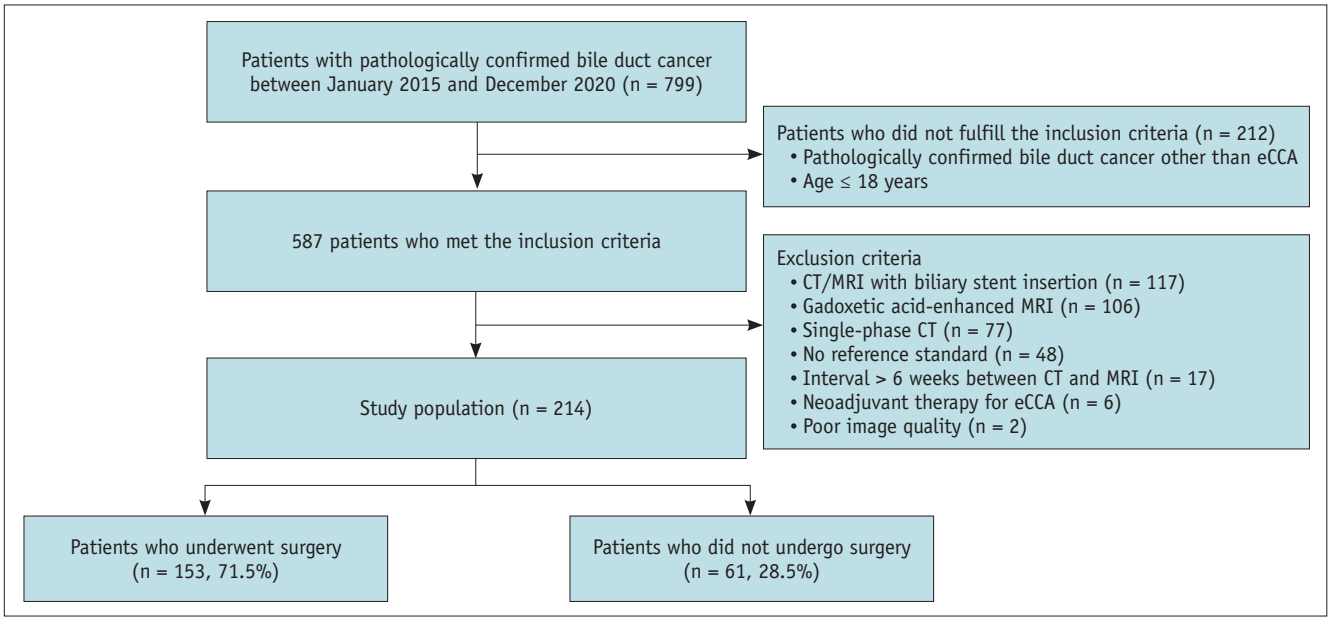

Fig. 1. Study flow. The final study population included 214 treatment-naïve patients with pathologically confirmed eCCA, who underwent both CECT and CE-MRI with MRCP using extracellular contrast media between January 2015 and December 2020. eCCA = extrahepatic cholangiocarcinoma, MRI = magnetic resonance imaging, CT = computed tomography, CECT = contrast-enhanced computed tomography, CE-MRI = contrast-enhanced magnetic resonance imaging, MRCP = magnetic resonance cholangiopancreatography

https://doi.org/10.3348/kjr.2023.0368

Korean Journal of Radiology
KJR

Table 1. Patient characteristics

Characteristics	Values
Sex	
Male	146 (68.2)
Female	68 (31.8)
Age, yr	68 ± 9
Tumor location	
Perihilar bile duct	121 (56.5)
Distal bile duct	93 (43.5)
Reference standard	
Surgical records and pathologic reports	153 (71.5)
MDT discussion-based clinical decision	61 (28.5)
Type of surgery	
Pylorus-preserving pancreaticoduodenectomy or Whipple's operation	77 (36.0)
RHH or extended RHH	34 (15.9)
Hilar resection or segmental bile duct resection	28 (13.1)
LHH or extended LHH	8 (3.7)
Hepaticopancreatoduodenectomy	4 (1.9)
Exploratory laparotomy	2 (0.9)
Not available due to clinically determined unresectability	61 (28.5)
Residual tumor	
R0	108 (50.5)
Non-R0 resection	45 (21.0)
Clinically unresectable	61 (28.5)
Pathologic T staging*	
Tis	2 (1.3)
T1	29 (19.2)
T2	86 (57.0)
T3	31 (20.5)
T4	3 (2.0)
Pathologic N staging*	
N0	82 (54.3)
N1	51 (33.8)
N2	12 (7.9)
Nx	6 (4.0)
Perineural invasion*	
Presence	123 (81.5)
Absence	28 (18.5)
Resection margin involved by high-grade dysplasia or carcinoma†	
Perihilar cholangiocarcinoma	25
Both proximal and distal bile duct	9 (36)
Proximal bile duct	8 (32)
Distal bile duct	5 (20)
Radial resection margin	1 (4)
Both distal bile duct and radial resection margin	1 (4)
Both proximal bile duct and radial resection margin	1 (4)
Distal cholangiocarcinoma	18
Proximal bile duct	11 (61.1)
Pancreas posterior margin	2 (11.1)
Distal bile duct	1 (5.6)
Pancreas anterior margin	1 (5.6)
Both proximal bile duct and pancreas posterior margin	1 (5.6)
Proximal bile duct and radial resection margin	1 (5.6)
Superior mesenteric artery groove	1 (5.6)
Interval between CECT and CE-MRI with MRCP, day	7 ± 11 (range, 0–42)
Interval between CECT and surgery, day‡	28 ± 18 (range, 1–60)
Interval between CE-MRI with MRCP and surgery, day‡	26 ± 17 (range, 1–60)

Data are number of patients with the percentage in parentheses or mean ± standard deviation unless otherwise indicated.
*Data are available in 151 patients who underwent curative-intent surgery, and the percentage values were calculated with 151 as the denominator, †Data are available in 43 patients (25 perihilar and 18 distal lesions) who had non-R0 resection margin after curative-intent surgery, and the percentage values were calculated with 25 and 18 as the denominators, ‡Data are available in 153 patients who underwent surgery.
MDT = multidisciplinary team, RHH = right hemihepatectomy, LHH = left hemihepatectomy, CECT = contrast-enhanced computed tomography, CE-MRI = contrast-enhanced magnetic resonance imaging, MRCP = magnetic resonance cholangiopancreatography

Among the 214 patients, 121 (56.5%) had perihilar CCA and 93 (43.5%) had distal CCA (Table 1). According to a multidisciplinary team-based decision, 61 (28.5%) patients were determined to have unresectable tumors. Moreover, 153 (71.5%) patients underwent surgery for eCCA, of which 151 patients underwent curative-intent surgery, while 2 patients underwent exploratory laparotomy only. R0 resection was achieved in 108/153 patients (70.6%). The reasons for unresectability in the 63 patients were local unresectability (n = 54) and distant metastasis to the lymph nodes (LNs) (n = 2), liver (n = 2), peritoneum (n = 2), both bone and distant LNs (n = 1), both liver and distant LNs (n = 1), and adrenal glands (n = 1).

Image Acquisition

CECT Imaging Protocol

All patients underwent multiphasic CT scans, including pre-contrast, arterial, and portal venous phases, using multidetector CT scanners with 64–320 channels: tube

https://doi.org/10.3348/kjr.2023.0368

voltage, 120 kVp; tube current, 150–250 mAs; slice thickness, 2–3 mm; and reconstruction interval, 0.6–5 mm (Supplementary Material).

CE-MRI with MRCP Protocol

CE-MRI with MRCP was performed using either 1.5 T (n = 20) or 3 T (n = 194) scanners. Heavily T2-weighted images, two-dimensional- and three-dimensional-MRCP images, pre-contrast T1-weighted images, dual-echo images, and diffusion-weighted images were obtained using b-values of 0 sec/mm^2 and 1000 sec/mm^2. The arterial, portal, and delayed phases were obtained after administering a standard dose of contrast medium (0.1 mmol/kg; Gadovist, Bayer) (Supplementary Material).

Image Analysis

Images were randomly distributed to reviewers, who were blinded to the clinical, surgical, and pathological information of the patients. The reviewers were only aware that CECT and CE-MRI with MRCP had been performed to determine eCCA. Four fellowship-trained radiologists, with 5, 6, 7, and 12 years of experience in abdominal imaging, respectively, independently reviewed both CECT and CE-MRI with MRCP data, including coronal and multiplanar reformatted images, and assessed the local tumor extent and distal metastasis to determine resectability. CECT was reviewed first, followed by CE-MRI with MRCP after an interval of > 4 weeks to minimize recall bias. The reviewers were asked to determine the Bismuth classification, tumor-vessel (celiac axis, hepatic artery, portal vein, superior mesenteric artery and vein, and inferior vena cava) relationship (no contact, abutment, or encasement), bile duct/vascular anatomic variations, perineural invasion, regional LN metastasis (absent, indeterminate, or present), and distant metastasis according to a recent KSAR consensus recommendation [6]. Regional LN metastasis was determined based on a short-axis diameter ≥ 10 mm and morphological features, such as round shape, heterogeneous enhancement, or central necrosis [6]. The presence of perineural invasion was considered when the tumor invaded the adjacent organs or adipose tissues or abutting or encasing vessels, or where there was soft tissue infiltration around the vessels not connected to the tumor [10,11]. Bismuth type IV classification with the tumor extending farther than the U or P point [12] and type III with contralateral vascular invasion or atrophy of the contralateral liver, atrophy of one hepatic lobe with contralateral vascular invasion, bilateral vessel involvement, main portal vein or proper hepatic artery involvement, or presence of distant metastasis were regarded as unresectable tumors. Tumor resectability was scored from 1 (definitely resectable) to 5 (definitely unresectable), and the reviewers were informed that scores of 3, 4, or 5 would be considered "unresectable" for statistical analysis.

One month after completing the CECT and CE-MRI analyses, the reviewers additionally reviewed the combined CECT and CE-MRI with MRCP set in cases showing discrepancies between the imaging modalities (e.g., resectability score of 1 or 2 on CECT and 4 or 5 on CE-MRI with MRCP) or with indeterminate resectability scores (score 3 on CECT or CE-MRI with MRCP).

Reference Standard

In patients who had undergone surgery, resectability was classified according to the surgical records and pathology reports as R0 (no residual tumor) or R1/2 (microscopic/macroscopic residual tumor). In cases where a patient did not undergo surgery owing to distant metastases and/or locally advanced cancer on preoperative imaging according to a multidisciplinary team-based consensus, the tumor was clinically confirmed as unresectable.

Statistical Analysis

Each reviewer's area under the receiver operating characteristic curve (AUC), sensitivity, specificity, positive predictive value (PPV), and negative predictive value (NPV) of CECT and CE-MRI with MRCP were compared using the z-test, McNemar test, and generalized estimating equation (GEE). The pooled AUC, sensitivity, specificity, PPV, and NPV of the two imaging modalities were compared using multi-reader, multi-case methods with random-reader models and GEE. For interobserver agreement, Fleiss kappa (κ) values were calculated and interpreted as follows: poor, < 0.20; fair, 0.20–0.39; moderate, 0.40–0.59; substantial, 0.60–0.79; and almost perfect, > 0.80 [13]. All statistical analyses were performed using SAS statistical software (SAS for Windows, version 9.4; SAS Institute), the MRMCaov package in the R 4.1.2 software (The R Foundation for Statistical Computing; https://github.com/brian-j-smith/MRMCaov), and MedCalc Statistical Software version 18.9.1 (MedCalc Software bvba); *P*-values < 0.05 were considered statistically significant.

https://doi.org/10.3348/kjr.2023.0368

Korean Journal of Radiology
KJR

RESULTS

CECT vs. CE-MRI with MRCP for Resectability Evaluation

When the presence of high-grade dysplasia at the resection margin was considered as R1 resection, no significant differences were observed between CECT and CE-MRI with MRCP in the pooled AUC (0.753 [95% confidence interval, 0.697–0.808] vs. 0.767 [0.720–0.814]), sensitivity (84.7% vs. 90.3%), specificity (52.6% vs. 51.4%), and PPV (64.6% vs. 65.4%) (P > 0.05 for all) (Table 2, Supplementary Table 1). The pooled NPV of CE-MRI with MRCP was significantly higher than that of CECT (83.8% vs. 77.2%, P = 0.033) (Figs. 2, 3).

When only the presence of invasive carcinoma at the resection margin was considered as R1 resection, no significant differences were observed between CECT and CE-MRI with MRCP in the pooled AUC (0.796 [0.743–0.848] vs. 0.791 [0.743–0.839]), sensitivity (85.3% vs. 89.7%), specificity (60.0% vs. 58.1%), PPV (74.6% vs. 74.7%), and NPV (74.7% vs. 80.4%) (P > 0.05 for all).

CECT Alone vs. Combined CECT and CE-MRI with MRCP when Assessing R0 Resectability in Patients with Discrepancies between Modalities or Indeterminate Findings

The reviewers additionally reviewed the combined CECT and CE-MRI with MRCP set in cases with discrepancies between imaging modalities (n = 26 [12.1%], n = 14 [6.5%], n = 26 [12.1%], and n = 23 [10.7%] for reviewers 1–4, respectively) or with indeterminate resectability scores (n = 3 [1.4%], n = 67 [31.3%], n = 49 [22.9%], and n = 28 [13.1%] for reviewers 1–4, respectively. The combined imaging set resulted in a significantly higher pooled AUC than that of CECT alone (0.798 [0.754–0.841] vs. 0.753 [0.697–0.808], P = 0.014) when determining R0 resectability (Table 3, Figs. 4, 5, Supplementary Table 2). Additionally, the combined imaging set showed significantly higher pooled PPV and NPV than those of CECT alone (PPV: 68.0% vs. 64.6%; NPV: 90.0% vs. 77.2%, P < 0.001 for both). In patients with perihilar CCA, subgroup analyses revealed that the combined imaging set had significantly higher PPV and NPV than those of CECT alone (P < 0.001 for both). In patients with distal CCA, the combined imaging set had a significantly higher NPV than that of CECT alone (P = 0.011) (Table 3). No significant differences in the pooled AUC, sensitivity, and specificity were observed between CE-MRI with MRCP and the combined imaging set (P > 0.05 for all).

CECT vs. CE-MRI with MRCP for Assessing the Local Tumor Extent

Among the 151 patients who underwent curative-intent surgery, non-R0 resection was performed in 45 patients (29.8%). These patients showed tumor presence in either the longitudinal (n = 25) or radial (n = 18) resection margins (Table 1). Perineural invasion was pathologically confirmed in 18.5% (28/151) of cases, and regional LN metastases were confirmed in 41.7% (63/151) of cases.

Longitudinal Tumor Extent

There were no significant differences in the pooled accuracy between CECT and CE-MRI with MRCP in determining

Table 2. Comparison of the diagnostic performance for resectability assessment in extrahepatic cholangiocarcinoma between CECT and CE-MRI with MRCP

Diagnostic performance	HGD regarded as R1 resection			HGD regarded as R0 resection		
	CECT	CE-MRI with MRCP	P	CECT	CE-MRI with MRCP	P
Pooled AUC	0.753 (0.697–0.808)	0.767 (0.720–0.814)	0.464	0.796 (0.743–0.848)	0.791 (0.743–0.839)	0.802
Pooled sensitivity*	84.7 (72.0–97.4) [366/432]	90.3 (85.9–94.6) [390/432]	0.206	85.3 (73.5–97.1) [423/496]	89.7 (84.7–94.8) [445/496]	0.174
Pooled specificity*	52.6 (43.1–62.1) [223/424]	51.4 (40.9–61.9) [218/424]	0.565	60.0 (50.8–69.2) [216/360]	58.1 (47.1–69.0) [209/360]	0.482
Pooled PPV*	64.6 (57.0–71.4) [366/567]	65.4 (58.0–72.2) [390/596]	0.506	74.6 (67.6–80.5) [423/567]	74.7 (67.8–80.5) [445/596]	0.965
Pooled NPV*	77.2 (69.1–83.6) [223/289]	83.8 (76.0–89.5) [218/260]	0.033†	74.7 (66.5–81.5) [216/289]	80.4 (71.9–86.8) [209/260]	0.076

Data in parentheses are 95% confidence intervals, and data in brackets are numbers of patients.
*Data are percentages, †P < 0.05.
CECT = contrast-enhanced computed tomography, CE-MRI = contrast-enhanced magnetic resonance imaging, MRCP = magnetic resonance cholangiopancreatography, HGD = high-grade dysplasia, AUC = area under the receiver operating characteristic curve, PPV = positive predictive value, NPV = negative predictive value.

https://doi.org/10.3348/kjr.2023.0368

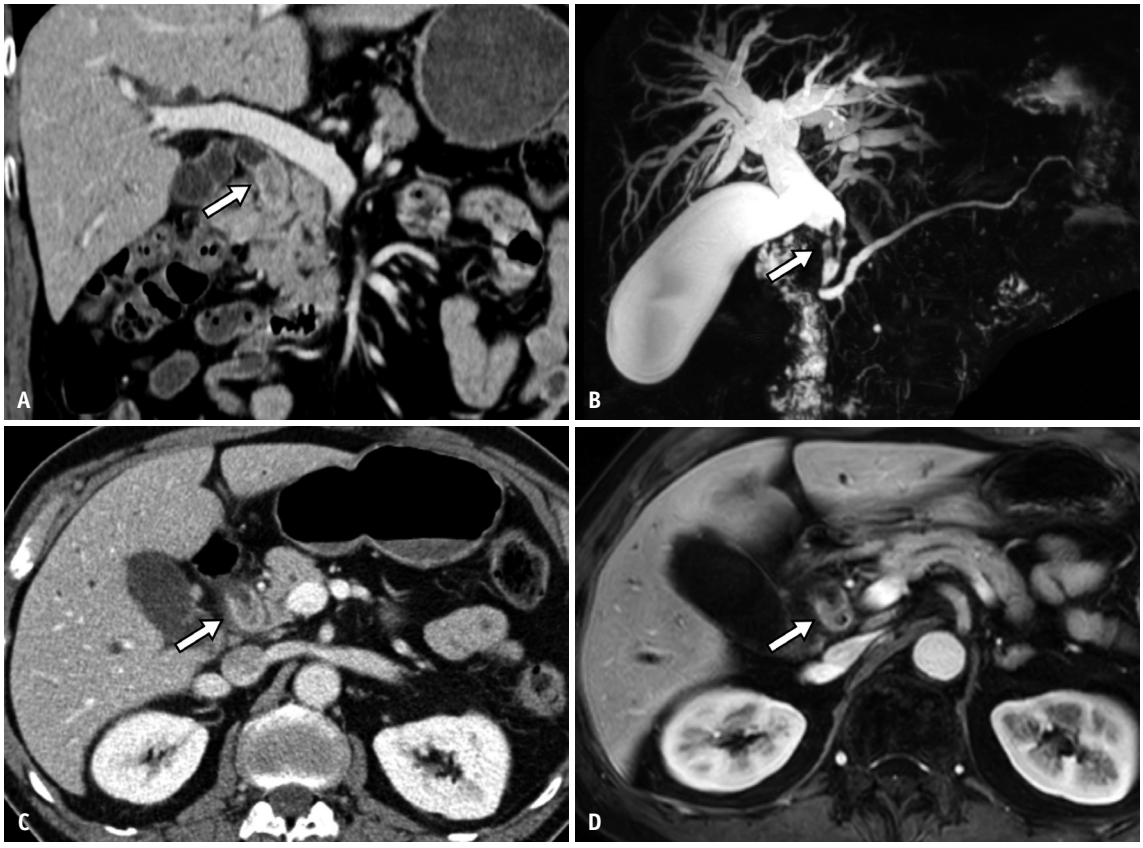

Fig. 2. A 77-year-old male patient with surgically confirmed distal cholangiocarcinoma with pathologic staging of T1N1. CECT coronal portal venous phase image **(A)** and three-dimensional MRCP **(B)** demonstrate distal CCA involving both the suprapancreatic and intrapancreatic common bile duct (arrows) with upstream bile duct dilatation. Axial portal venous phase images of CECT **(C)** and CE-MRI **(D)** show that the tumor (arrows) does not contact the hepatic artery or portal vein. On both CT and MRI, distal CCA was assessed as "probably" or "definitely" resectable. The patient underwent the Whipple operation, and histopathologic analysis revealed adenocarcinoma with a tumor-free resection margin. CECT = contrast-enhanced computed tomography, MRCP = magnetic resonance cholangiopancreatography, CCA = cholangiocarcinoma, CE-MRI = contrast-enhanced magnetic resonance imaging, MRI = magnetic resonance imaging, CT = computed tomography

the tumor involvement of the bilateral secondary confluence (65.7% vs. 65.0%; $P = 0.624$), primary confluence (85.4% vs. 71.4%; $P = 0.337$), and intrapancreatic common bile duct (CBD) (75.5% vs. 73.3%; $P = 0.148$) (Table 4). The Bismuth classification determined on both imaging modalities by each reviewer is described in Supplementary Table 3.

Vascular Invasion

When only encasement on imaging was considered as vascular invasion, the pooled accuracy of CECT and CE-MRI with MRCP was 88.2%–97.8% and 85.1%–97.2%, respectively, with no significant difference ($P > 0.05$ for all) (Table 4). When both abutment and encasement on imaging were considered as vascular invasion, the pooled accuracy of CECT and CE-MRI with MRCP was 63.7%–96.2% and 63.2%–95.7%, respectively, with no significant difference ($P > 0.05$ for all) (Supplementary Table 4). The accuracy and specificity for diagnosing vascular invasion were significantly higher when only encasement on imaging was considered as vascular invasion rather than both abutment and encasement ($P < 0.05$ for all) (Fig. 6, Supplementary Table 5).

Perineural Invasion and Regional LN Metastasis

The pooled accuracy of CECT and CE-MRI with MRCP in assessing perineural invasion was 58.4% and 57.9%, respectively, with no significant difference ($P = 0.762$) (Table 4). When both indeterminate and metastatic LNs on imaging were considered metastatic for statistical analysis, the pooled accuracy of CECT and CE-MRI with MRCP in determining regional LN metastasis was 58.4% and 59.3%, respectively, without a significant difference ($P = 0.769$) (Table 4). Data from each reviewer are described in the Supplementary Material.

https://doi.org/10.3348/kjr.2023.0368

Korean Journal of Radiology
KJR

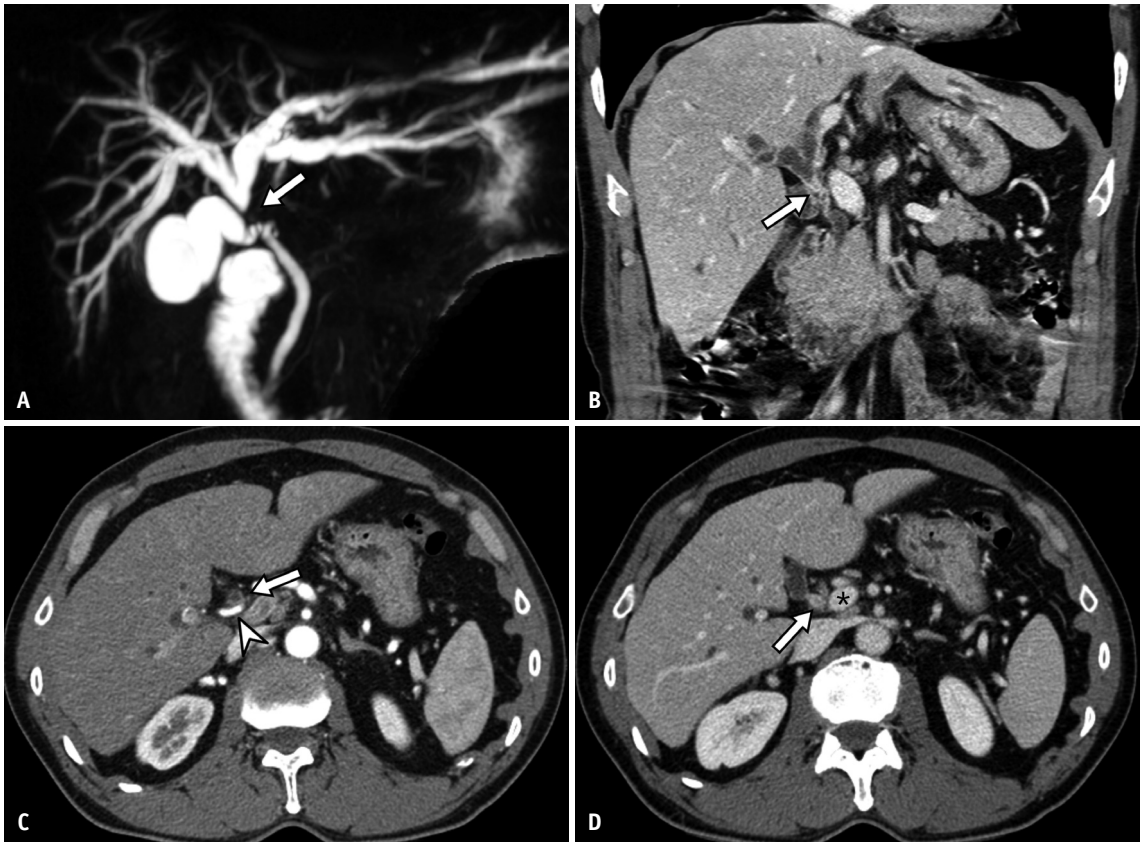

Fig. 3. A 62-year-old male patient with surgically confirmed perihilar cholangiocarcinoma with pathologic staging of T2aN0. Three-dimensional MRCP **(A)** and CECT coronal portal venous phase image **(B)** demonstrate Bismuth type I CCA (arrows) and mild upstream bile duct dilatation. Axial arterial **(C)** and portal venous phase **(D)** images show that the tumor (arrows) does not encase the hepatic artery (**C**, arrowhead) and portal vein (**D**, asterisk). The tumor was assessed as "probably" or "definitely" resectable on both imaging modalities. However, after curative-intent hilar resection, tumor presence was observed in the right secondary confluence and left hepatic duct resection margin. MRCP = magnetic resonance cholangiopancreatography, CECT = contrast-enhanced computed tomography, CCA = cholangiocarcinoma

Interobserver Agreement

The interobserver agreement for overall resectability among the four reviewers was fair for both CECT (κ = 0.323) and CE-MRI with MRCP (κ = 0.320), without a significant difference (P = 0.884) (Supplementary Table 6). The interobserver agreement of CECT was significantly higher than that of CE-MRI with MRCP for suprapancreatic (κ = 0.548 vs. κ = 0.364, P < 0.001) and intrapancreatic CBD involvement (κ = 0.680 vs. κ = 0.570, P = 0.004), as well as for tumor-vessel relationship for the main portal vein (κ = 0.365 vs. κ = 0.273, P = 0.036). Regarding the Bismuth classification, both CECT (κ = 0.530) and CE-MRI with MRCP (κ = 0.510) showed moderate agreement, without a significant difference (P = 0.084).

DISCUSSION

In our study, CECT and CE-MRI with MRCP did not differ significantly in the AUC, sensitivity, and specificity for determining the R0 resectability of eCCA. Additionally, subgroup analyses revealed no significant differences in the diagnostic performance of these two imaging modalities when assessing the tumor extent and tumor-vessel relationships. The nonsignificant difference in determining R0 resectability between these two imaging modalities could be attributed to various reasons. First, multiplanar and maximum intensity projection CECT images helped evaluate the longitudinal tumor extent and bile duct anatomical variations, potentially replacing the role of MRCP. Second, we might have depended heavily on T1-weighted dynamic sequences when determining the tumor-vessel relationship and longitudinal extent of the eCCA with CE-MRI, and these sequences exhibit essentially the same features as CECT. Lastly, the superior soft tissue contrast of MRI may play a limited role because of the small size of the

 https://doi.org/10.3348/kjr.2023.0368

Table 3. Comparison of diagnostic performance for R0 resectability in patients with discrepancies between modalities or indeterminate findings in CECT, CE-MRI with MRCP, and combined CECT and CE-MRI with MRCP

Diagnostic performance	CECT (A)	CE-MRI with MRCP (B)	Combined CECT and CE-MRI with MRCP (C)	*P*-value† (A vs. C)	*P*-value† (B vs. C)
All types of cancer (n = 214)					
Pooled AUC	0.753 (0.697–0.808)	0.767 (0.720–0.814)	0.798 (0.754–0.841)	0.014‡	0.078
Pooled sensitivity*	84.7 (72.0–97.4) [366/432]	90.3 (85.9–94.6) [390/432]	94.0 (87.9–100.0) [406/432]	0.036	0.339
Pooled specificity*	52.6 (43.1–62.1) [223/424]	51.4 (40.9–61.9) [218/424]	55.0 (46.2–63.7) [233/424]	0.260	0.104
Pooled PPV*	64.6 (57.0–71.4) [366/567]	65.4 (58.0–72.2) [390/596]	68.0 (60.6–74.6) [406/597]	< 0.001‡	0.010‡
Pooled NPV*	77.2 (69.1–83.6) [223/289]	83.8 (76.0–89.5) [218/260]	90.0 (83.6–94.0) [233/259]	< 0.001‡	0.022
Perihilar bile duct cancer (n = 121)					
Pooled AUC	0.686 (0.604–0.768)	0.730 (0.675–0.784)	0.776 (0.725–0.826)	0.047	0.054
Pooled sensitivity*	70.3 (45.1–95.6) [121/172]	81.4 (70.0–92.8) [140/172]	87.8 (71.5–100.0) [151/172]	0.127	0.315
Pooled specificity*	59.6 (49.0–70.2) [186/312]	59.6 (47.9–71.4) [186/312]	62.8 (53.6–72.1) [196/312]	0.287	0.127
Pooled PPV*	49.0 (38.2–59.9) [121/247]	52.6 (41.8–63.2) [140/266]	56.6 (45.6–66.9) [151/267]	< 0.001‡	0.025
Pooled NPV*	78.5 (69.3–85.5) [186/237]	85.3 (76.9–91.0) [186/218]	90.3 (83.1–94.6) [196/217]	< 0.001‡	0.077
Distal bile duct cancer (n = 93)					
Pooled AUC	0.691 (0.599–0.783)	0.681 (0.591–0.771)	0.713 (0.617–0.808)	0.231	0.292
Pooled sensitivity*	94.2 (88.4–100.0) [245/260]	96.2 (93.4–98.9) [250/260]	98.1 (96.6–99.5) [255/260]	0.155	0.140
Pooled specificity*	33.0 (18.5–47.6) [37/112]	28.6 (11.5–45.6) [32/112]	33.0 (16.8–49.3) [37/112]	1.000	0.424
Pooled PPV*	76.6 (66.5–84.3) [245/320]	75.8 (65.7–83.6) [250/330]	77.3 (67.3–84.9) [255/330]	0.365	0.189
Pooled NPV*	71.2 (52.2–84.8) [37/52]	76.2 (52.1–90.4) [32/42]	88.1 (69.0–96.1) [37/42]	0.011‡	0.099

Data in parentheses are 95% confidence intervals, and data in brackets are numbers of patients.
*Data are percentages, †*P*-value < 0.016 indicates statistically significant difference, ‡*P* < 0.016.
CECT = contrast-enhanced computed tomography, CE-MRI = contrast-enhanced magnetic resonance imaging, MRCP = magnetic resonance cholangiopancreatography, AUC = area under the receiver operating characteristic curve, PPV = positive predictive value, NPV = negative predictive value

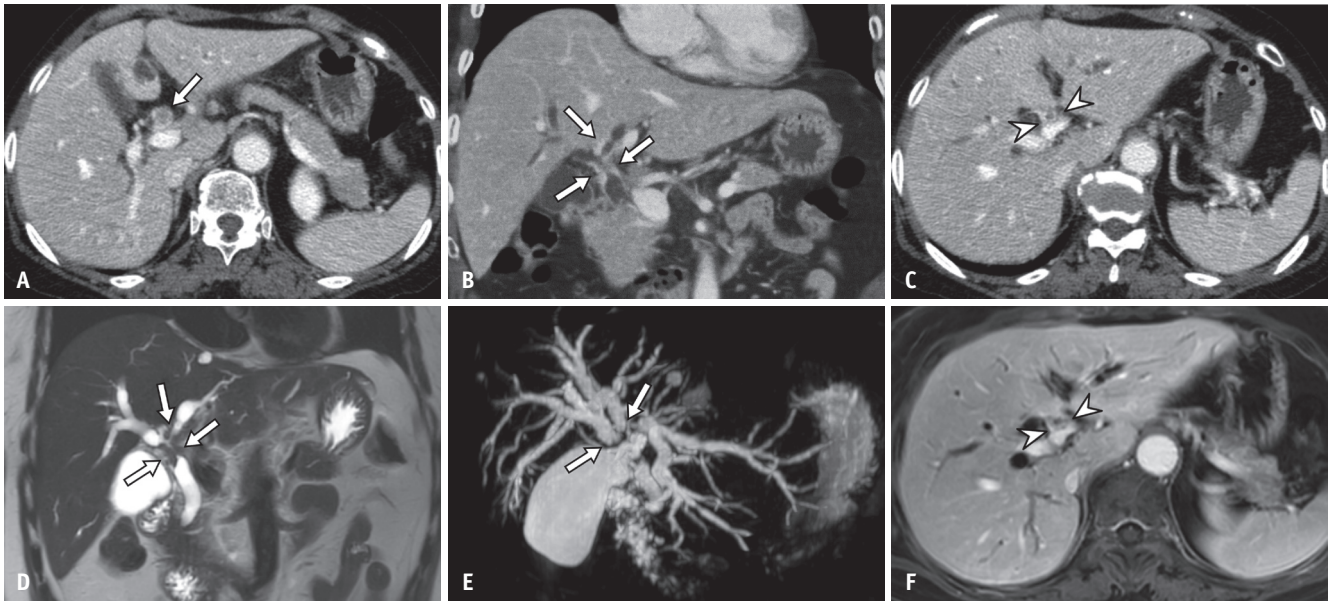

Fig. 4. A 69-year-old female patient with surgically confirmed perihilar cholangiocarcinoma with pathologic staging of T4N2. Axial **(A, C)** and coronal **(B)** portal venous phase CT images reveal wall thickening and enhancement of the common hepatic duct and left hepatic duct (**A, B**, arrows) abutting the left portal vein (**C**, arrowheads). On CT, the tumor was classified as Bismuth type II or IIIb with probable resectability. On coronal T2-weighted **(D)** and MRCP **(E)** images of CE-MRI with MRCP, ductal wall thickening is seen in the common hepatic duct, left hepatic duct (**D**, arrows), and right secondary confluence separation (**E**, arrows). The axial portal venous phase image **(F)** shows luminal narrowing of the left portal vein (arrowheads). The reviewers assessed this case as "probably" unresectable with Bismuth type IV classification on MRI and combined review of CECT and CE-MRI with MRCP. The patient underwent an extended right hemihepatectomy, and the tumor involved the surgical margin at the left secondary confluence and bile duct radial margin. CT = computed tomography, MRCP = magnetic resonance cholangiopancreatography, CE-MRI = contrast-enhanced magnetic resonance imaging, MRI = magnetic resonance imaging, CECT = contrast-enhanced computed tomography

https://doi.org/10.3348/kjr.2023.0368

Korean Journal of Radiology
KJR

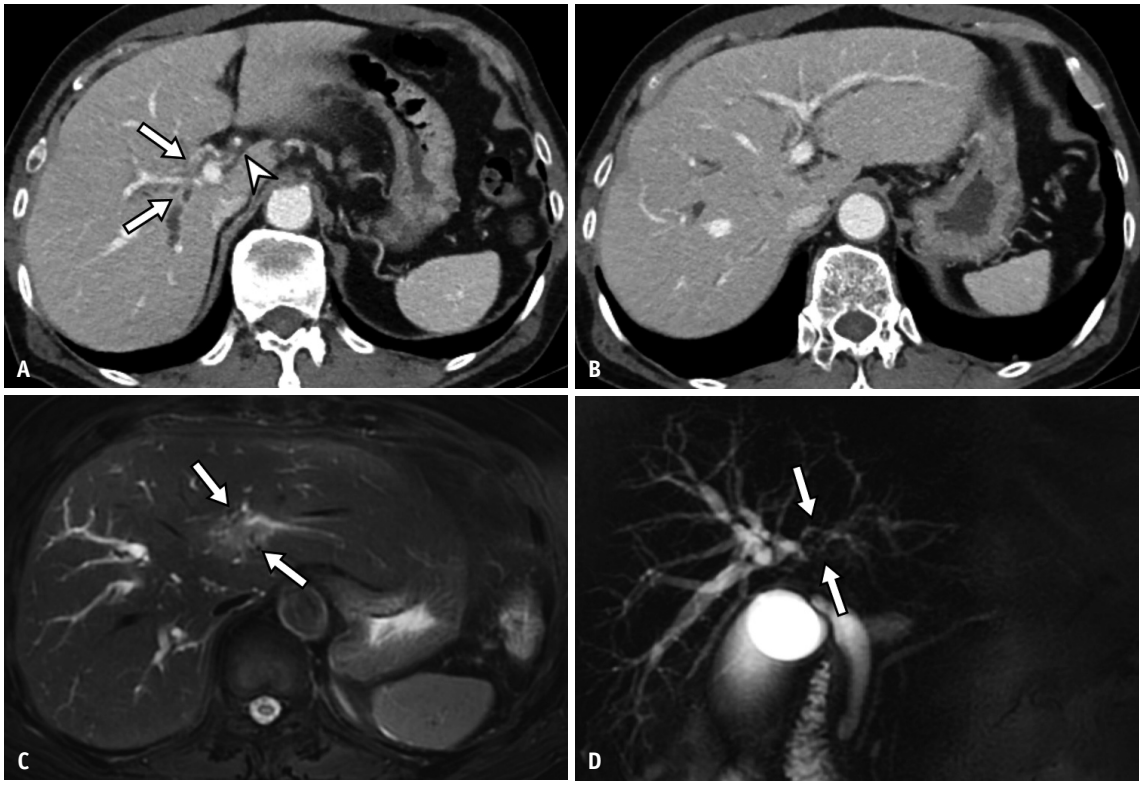

Fig. 5. A 66-year-old male patient with biopsy-confirmed perihilar cholangiocarcinoma. On CECT, axial portal venous phase images **(A, B)** show wall thickening and enhancement of the common hepatic duct and right secondary confluence (**A**, arrows) and soft tissue around the right hepatic artery (**A**, arrowhead). **B:** The left hepatic duct is minimally dilated, and the secondary confluence separation is not evident. Two reviewers rated this case as "indeterminate" resectability, while the other reviewers rated it as "probably" unresectable. On CE-MRI with MRCP, which was performed 12 days later, the axial T2-weighted and MRCP images **(C, D)** of CE-MRI with MRCP show the tumor involving the left secondary confluence as well (arrows). All reviewers determined this case as "definitely" unresectable on both CE-MRI with MRCP and the combined review of CECT and CE-MRI with MRCP. The patient did not undergo surgery based on the decision made in the multidisciplinary team conference. CECT = contrast-enhanced computed tomography, CE-MRI = contrast-enhanced magnetic resonance imaging, MRCP = magnetic resonance cholangiopancreatography

structures involved in eCCA, whereas CECT could still have the potential advantage of spatial resolution. Our findings are consistent with those of previous studies that reported no significant difference between CECT and CE-MRI with MRCP in resectability determination [7-9]. Nonetheless, in indeterminate or inconsistent cases of resectability determination, the combined review of CECT and CE-MRI with MRCP showed significant improvements in the PPV and NPV and a marginal improvement in the AUC when compared with CECT alone, particularly in the perihilar CCA subgroup. Thus, we cautiously propose that additional CE-MRI with MRCP may be beneficial, especially in patients with perihilar CCA, when R0 resectability is not evident on CECT alone. Our results also support the recent KSAR statement that recommends CECT as the initial and standard imaging modality and CE-MRI with MRCP as an alternative to CECT [6].

In our study, the pooled specificities of CECT and CE-MRI with MRCP were 52.6% and 51.4%, respectively, while the pooled sensitivities were 84.7% and 90.3%, respectively. This is consistent with previous studies showing modest specificity for CECT (11.1%–75.9%) [14-16] and CE-MRI with MRCP (60%–71.5%) [7,17,18]. The relatively high sensitivity and low specificity of both imaging modalities could be due to underestimation of the tumor extent, which could be attributed to the longitudinal spread of eCCA along the bile duct wall with microscopic submucosal extension [1]. Even when only the presence of a gross tumor at the resection margin was considered as R1 resection, the modest specificity did not improve for either imaging modality. According to our observations, detecting microscopic tumor spread along the mucosa or submucosa remains a challenging endeavor [1,19] for both imaging modalities, owing to limited spatial and/or contrast resolution. Consequently, reports on longitudinal tumor extent should consider the length of undetectable

 https://doi.org/10.3348/kjr.2023.0368

Table 4. Comparing diagnostic performance between CECT and CE-MRI with MRCP for assessing extrahepatic cholangiocarcinoma extent and tumor-vessel relationship

Diagnostic performance	CECT	CE-MRI with MRCP	*P*
Secondary confluence involvement			
Pooled accuracy	65.7 (59.9–71.5) [562/856]	65.0 (59.3–70.6) [556/856]	0.624
Pooled sensitivity	79.4 (65.1–93.7) [143/180]	76.7 (50.8–100.0) [138/180]	0.661
Pooled specificity	62.0 (55.0–69.0) [419/676]	61.8 (54.9–68.8) [418/676]	0.898
Pooled PPV	35.8 (27.3–45.2) [143/400]	34.8 (26.7–44.0) [138/396]	0.593
Pooled NPV	91.9 (86.5–95.2) [419/456]	90.9 (86.0–94.2) [418/460]	0.571
Primary confluence involvement			
Pooled accuracy	85.4 (81.0–89.9) [516/604]	71.4 (31.6–100.0) [431/604]	0.337
Pooled sensitivity	76.6 (67.0–86.1) [196/256]	67.6 (23.7–100.0) [173/256]	0.564
Pooled specificity	92.0 (86.7–97.2) [320/348]	74.1 (36.7–100.0) [258/348]	0.214
Pooled PPV	87.5 (78.3–93.1) [196/224]	65.8 (57.1–73.5) [173/263]	< 0.001*
Pooled NPV	84.2 (76.4–89.8) [320/380]	75.7 (68.0–82.0) [258/341]	0.001*
Intrapancreatic CBD involvement			
Pooled accuracy	75.5 (70.1–80.9) [456/604]	73.3 (68.2–78.5) [443/604]	0.148
Pooled sensitivity	70.6 (59.8–81.4) [223/316]	63.3 (54.3–72.3) [200/316]	0.105
Pooled specificity	80.9 (72.5–89.3) [233/288]	84.4 (76.2–92.5) [243/288]	0.400
Pooled PPV	80.2 (70.8–87.1) [223/278]	81.6 (73.4–87.8) [200/245]	0.550
Pooled NPV	71.5 (61.8–79.5) [233/326]	67.7 (58.3–75.8) [243/359]	0.045*
HA invasion			
Pooled accuracy	47.5 (41.1–54.0) [407/856]	47.4 (41.0–53.8) [406/856]	0.905
Pooled sensitivity	91.7 (65.1–100.0) [11/12]	91.7 (65.1–100.0) [11/12]	1.000
Pooled specificity	46.9 (40.3–53.6) [396/844]	46.8 (40.4–53.2) [395/844]	0.905
Pooled PPV	2.4 (0.8–7.2) [11/459]	2.4 (0.8–7.2) [11/460]	0.987
Pooled NPV	99.7 (98.2–100.0) [396/397]	99.7 (98.2–100.0) [395/396]	0.999
PV invasion			
Pooled accuracy	96.0 (93.5–98.6) [580/604]	96.7 (94.6–98.8) [584/604]	0.391
Pooled sensitivity	50.0 (3.1–96.9) [8/16]	68.8 (22.3–100.0) [11/16]	0.242
Pooled specificity	97.3 (94.4–100.0) [572/588]	97.4 (95.2–99.7) [573/588]	0.824
Pooled PPV	33.3 (11.0–66.9) [8/24]	42.3 (17.0–72.4) [11/26]	0.248
Pooled NPV	98.6 (95.3–99.6) [572/580]	99.1 (95.8–99.8) [573/578]	0.201
Perineural invasion			
Pooled accuracy	58.4 (33.9–83.0) [353/604]	57.9 (36.0–79.9) [350/604]	0.762
Pooled sensitivity	58.9 (22.1–95.8) [290/492]	57.7 (22.0–93.5) [284/492]	0.103
Pooled specificity	56.3 (27.4–85.1) [63/112]	58.9 (21.8–96.0) [66/112]	0.756
Pooled PPV	85.5 (78.2–90.7) [290/339]	86.1 (78.9–91.1) [284/330]	0.764
Pooled NPV	23.8 (16.2–33.5) [63/265]	24.1 (16.5–33.7) [66/274]	0.880
Regional LN metastasis			
Pooled accuracy	58.4 (52.8–64.1) [339/580]	59.3 (53.6–65.0) [344/580]	0.769
Pooled sensitivity	36.1 (9.9–62.3) [91/252]	24.2 (0.0–50.4) [61/252]	0.082
Pooled specificity	75.6 (46.5–100.0) [248/328]	86.3 (67.2–100.0) [283/328]	0.104
Pooled PPV	53.2 (42.2–63.9) [91/171]	57.5 (44.9–69.3) [61/106]	0.436
Pooled NPV	60.6 (51.9–68.7) [248/409]	59.7 (51.3–67.6) [283/474]	0.613

Data are percentages with the 95% confidence interval in parentheses and numbers of patients in brackets.
*$P < 0.05$.
CECT = contrast-enhanced computed tomography, CE-MRI = contrast-enhanced magnetic resonance imaging, MRCP = magnetic resonance cholangiopancreatography, PPV = positive predictive value, NPV = negative predictive value, CBD = common bile duct, HA = hepatic artery, PV = portal vein, LN = lymph node

https://doi.org/10.3348/kjr.2023.0368

Korean Journal of Radiology
KJR

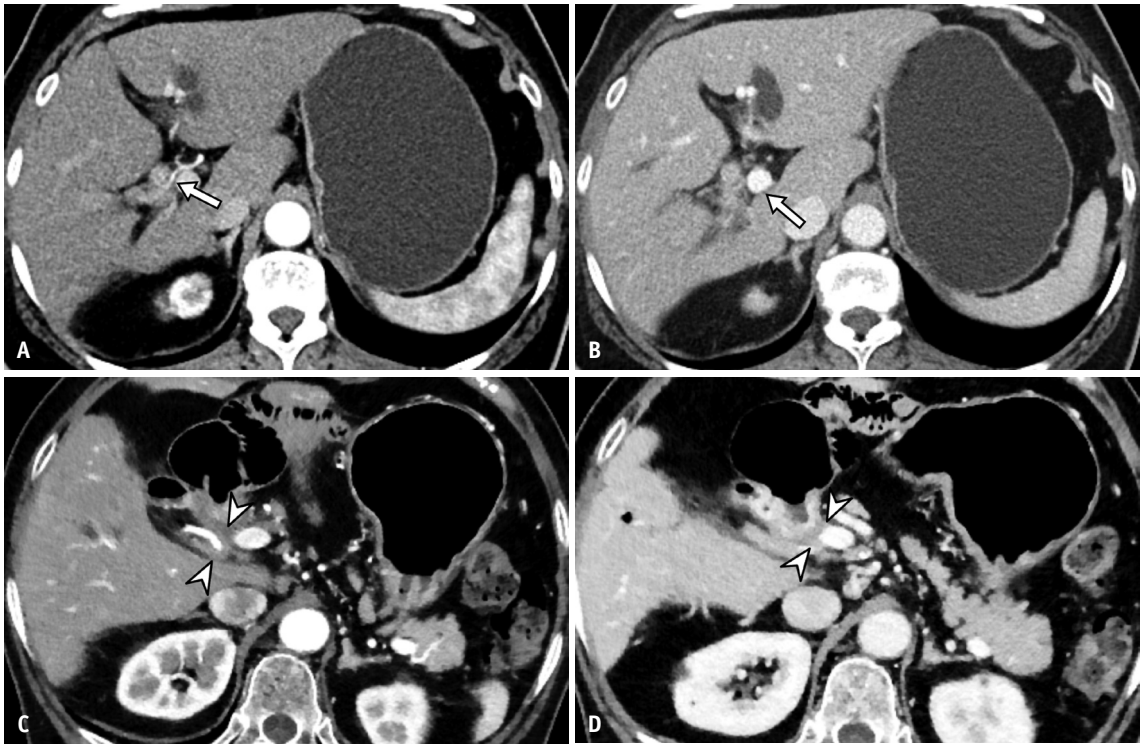

Fig. 6. Tumor-vessel relationship on imaging. **A, B:** A 68-year-old female patient with perihilar cholangiocarcinoma. Arterial **(A)** and portal venous phase **(B)** images show the right hepatic artery (**A**, arrow) and portal vein (**B**, arrow) abutting the Bismuth type IV CCA. The absence of vascular invasion was confirmed after extended right hemihepatectomy. **C, D:** A 71-year-old female patient with distal common bile duct cancer. Axial arterial **(C)** and portal venous phase **(D)** images show encasement of the right hepatic artery from the superior mesenteric artery (**C**, arrowheads) and main portal vein encasement with minimal luminal deformity (**D**, arrowheads). Both arterial and portal invasions were confirmed after the Whipple operation. CCA = cholangiocarcinoma

mucosal or submucosal spread.

We also evaluated the tumor-vessel relationship, perineural invasion, and regional LN metastasis. The pooled accuracy of vascular invasion was 85.1%–97.8% for the two modalities, without a significant difference. Our findings corroborate those of previous studies that demonstrated the high diagnostic performance of both CECT and CE-MRI with MRCP in assessing vascular involvement [7,17,20,21]. Adopting less stringent criteria for vascular invasion in our study led to reduced accuracy and specificity of both CECT and CE-MRI with MRCP. Our results are consistent with those of a recent study [22] that reported a high PPV for vascular invasion using the encasement criterion. Since the prevalence of vascular invasion is low among surgical candidates with eCCA [14], as observed in our study, using vascular invasion criteria with high specificity would lead to high accuracy in identifying potential candidates for curative-intent surgery. While acknowledging the potential decrease in sensitivity, we believe that using encasement as the sole criterion for vascular invasion can still contribute to the precise assessment of eCCA resectability. Regarding perineural invasion, both imaging modalities showed high PPVs (80.2%–81.6%), indicating a high likelihood of pathologic confirmation of perineural invasion when it is suspected on imaging. In contrast, both imaging modalities demonstrated low sensitivity (24.2%–36.1%) in determining regional LN metastasis, as previously reported [14,15]. The conventional criteria of short-axis diameter and morphological features [6] might not be sufficient for accurate LN staging, and caution is required to avoid overlooking small LNs in clinical practice.

With an increased emphasis on multidisciplinary collaboration for the management of eCCA [23], interobserver agreement in determining resectability would be even more critical, since the radiologists' consensus on resectability would affect the treatment plan. In our study, CT demonstrated better interobserver agreement than CE-MRI in terms of suprapancreatic and intrapancreatic CBD involvement and the tumor-vessel relationship of the main portal vein. This may be due to the lower number of phases in CECT compared to CE-MRI and the availability of multiplanar images with high spatial resolution, which enables reliable image interpretation. Our study results also support the KSAR

 https://doi.org/10.3348/kjr.2023.0368

statement recommending CECT as the initial and standard imaging modality, rather than CE-MRI with MRCP. However, our study revealed that both imaging modalities provided only fair interobserver agreement regarding overall resectability, which is inconsistent with a recent report [14] showing that structural reports increased interobserver agreement. We suggest that definitions for the lexicon and standardized terminology should also be added to eCCA to improve interobserver agreement regarding the resectability criteria.

Our study has several limitations. First, owing to its retrospective design, selection bias was unavoidable. Second, we included some patients with unresectable eCCA based on a multidisciplinary conference discussion that already included imaging-based decision-making. This may have led to an overestimation of the diagnostic performance of the imaging modalities. In contrast, only patients who underwent curative-intent surgery were included for radiologic-pathological comparison. Therefore, the performance of both imaging modalities may have been underestimated in the assessment of longitudinal and radial tumor extents. Third, the image quality of CE-MRI with MRCP might vary between machines with different field strengths, which can affect diagnostic performance. Lastly, because the interpretation of the combined imaging set is far more common than that of CE-MRI alone in routine clinical practice, a comparison of the combined imaging set with CE-MRI in our study might not have been pragmatic.

In conclusion, CECT and CE-MRI with MRCP did not differ significantly in their AUC, sensitivity, specificity, or interobserver agreement regarding the assessment of the resectability of eCCA. Furthermore, the addition of CE-MRI to MRCP increased the diagnostic performance of CECT, when R0 resectability was not evident on CECT alone. The interobserver agreement of both CT and CE-MRI with MRCP for determining the resectability was fair.

Supplement

The Supplement is available with this article at https://doi.org/10.3348/kjr.2023.0368.

Availability of Data and Material

The datasets generated or analyzed during the study are available from the corresponding author on reasonable request.

Conflicts of Interest

Jeong Min Lee, the editor board member of the *Korean Journal of Radiology*, was not involved in the editorial evaluation or decision to publish this article. All authors have declared no conflicts of interest.

Author Contributions

Conceptualization: Jeong Hee Yoon. Data curation: Jeongin Yoo. Formal analysis: Jeongin Yoo. Funding acquisition: Jeong Hee Yoon. Investigation: Hyo-Jin Kang, Jae Seok Bae, Sun Kyung Jeon. Methodology: Jeong Hee Yoon. Project administration: Jeong Hee Yoon, Jeong Min Lee. Resources: Jeong Hee Yoon. Software: Jeong Hee Yoon. Supervision: Jeong Hee Yoon. Validation: Jeongin Yoo, Jeong Hee Yoon. Visualization: Jeongin Yoo, Jeong Hee Yoon. Writing—original draft: Jeongin Yoo, Jeong Hee Yoon. Writing—review & editing: all authors.

ORCID IDs

Jeongin Yoo
https://orcid.org/0000-0002-3267-2544
Jeong Min Lee
https://orcid.org/0000-0003-0561-8777
Hyo-Jin Kang
https://orcid.org/0000-0002-6771-2112
Jae Seok Bae
https://orcid.org/0000-0003-2768-7917
Sun Kyung Jeon
https://orcid.org/0000-0002-8991-3986
Jeong Hee Yoon
https://orcid.org/0000-0002-9925-9973

Funding Statement

This research was supported by the Bio & Medical Technology Development Program of the National Research Foundation (NRF) funded by the Korean government (MSIT) (NRF-2021R1C1C1004569) and the National R&D Program for Cancer Control through the National Cancer Center (NCC) funded by the Ministry of Health & Welfare, Republic of Korea (HA21C0143000021).

Acknowledgments

We appreciate the statistical advice from the Medical Research Collaborating Center at Seoul National University Hospital and Seoul National University College of Medicine.

Korean Journal of Radiology
KJR

REFERENCES

1. Joo I, Lee JM, Yoon JH. Imaging diagnosis of intrahepatic and perihilar cholangiocarcinoma: recent advances and challenges. *Radiology* 2018;288:7-13
2. Valle JW, Borbath I, Khan SA, Huguet F, Gruenberger T, Arnold D; ESMO Guidelines Committee. Biliary cancer: ESMO clinical practice guidelines for diagnosis, treatment and follow-up. *Ann Oncol* 2016;27(suppl 5):v28-v37
3. Klempnauer J, Ridder GJ, Werner M, Weimann A, Pichlmayr R. What constitutes long-term survival after surgery for hilar cholangiocarcinoma? *Cancer* 1997;79:26-34
4. Blechacz B, Komuta M, Roskams T, Gores GJ. Clinical diagnosis and staging of cholangiocarcinoma. *Nat Rev Gastroenterol Hepatol* 2011;8:512-522
5. Ruys AT, van Beem BE, Engelbrecht MR, Bipat S, Stoker J, Van Gulik TM. Radiological staging in patients with hilar cholangiocarcinoma: a systematic review and meta-analysis. *Br J Radiol* 2012;85:1255-1262
6. Lee DH, Kim B, Lee ES, Kim HJ, Min JH, Lee JM, et al. Radiologic evaluation and structured reporting form for extrahepatic bile duct cancer: 2019 consensus recommendations from the Korean Society of Abdominal Radiology. *Korean J Radiol* 2021;22:41-62
7. Park HS, Lee JM, Choi JY, Lee MW, Kim HJ, Han JK, et al. Preoperative evaluation of bile duct cancer: MRI combined with MR cholangiopancreatography versus MDCT with direct cholangiography. *AJR Am J Roentgenol* 2008;190:396-405
8. Ryoo I, Lee JM, Park HS, Han JK, Choi BI. Preoperative assessment of longitudinal extent of bile duct cancers using MDCT with multiplanar reconstruction and minimum intensity projections: comparison with MR cholangiography. *Eur J Radiol* 2012;81:2020-2026
9. D'Antuono F, De Luca S, Mainenti PP, Mollica C, Camera L, Galizia G, et al. Comparison between multidetector CT and high-field 3T MR imaging in diagnostic and tumour extension evaluation of patients with cholangiocarcinoma. *J Gastrointest Cancer* 2020;51:534-544
10. Raghavan K, Jeffrey RB, Patel BN, DiMaio MA, Willmann JK, Olcott EW. MDCT diagnosis of perineural invasion involving the celiac plexus in intrahepatic cholangiocarcinoma: preliminary observations and clinical implications. *AJR Am J Roentgenol* 2015;205:W578-W584
11. Yamada Y, Mori H, Hijiya N, Matsumoto S, Takaji R, Kiyonaga M, et al. Extrahepatic bile duct cancer: invasion of the posterior hepatic plexuses--evaluation using multidetector CT. *Radiology* 2012;263:419-428
12. Takayasu K, Moriyama N, Muramatsu Y, Shima Y, Goto H, Yamada T. Intrahepatic portal vein branches studied by percutaneous transhepatic portography. *Radiology* 1985;154:31-36
13. Viera AJ, Garrett JM. Understanding interobserver agreement: the kappa statistic. *Fam Med* 2005;37:360-363
14. Lee DH, Kim B, Lee JM, Lee ES, Choi MH, Kim H. Multidetector CT of extrahepatic bile duct cancer: diagnostic performance of tumor resectability and interreader agreement. *Radiology* 2022;304:96-105
15. Ni Q, Wang H, Zhang Y, Qian L, Chi J, Liang X, et al. MDCT assessment of resectability in hilar cholangiocarcinoma. *Abdom Radiol (NY)* 2017;42:851-860
16. Nagakawa Y, Kasuya K, Bunso K, Hosokawa Y, Kuwabara H, Nakagima T, et al. Usefulness of multi-3-dimensional computed tomograms fused with multiplanar reconstruction images and peroral cholangioscopy findings in hilar cholangiocarcinoma. *J Hepatobiliary Pancreat Sci* 2014;21:256-262
17. Ryoo I, Lee JM, Chung YE, Park HS, Kim SH, Han JK, et al. Gadobutrol-enhanced, three-dimensional, dynamic MR imaging with MR cholangiography for the preoperative evaluation of bile duct cancer. *Invest Radiol* 2010;45:217-224
18. Kim JY, Kim MH, Lee TY, Hwang CY, Kim JS, Yun SC, et al. Clinical role of 18F-FDG PET-CT in suspected and potentially operable cholangiocarcinoma: a prospective study compared with conventional imaging. *Am J Gastroenterol* 2008;103:1145-1151
19. Sakamoto E, Nimura Y, Hayakawa N, Kamiya J, Kondo S, Nagino M, et al. The pattern of infiltration at the proximal border of hilar bile duct carcinoma: a histologic analysis of 62 resected cases. *Ann Surg* 1998;227:405-411
20. Choi JY, Lee JM, Lee JY, Kim SH, Lee MW, Han JK, et al. Assessment of hilar and extrahepatic bile duct cancer using multidetector CT: value of adding multiplanar reformations to standard axial images. *Eur Radiol* 2007;17:3130-3138
21. Lee HY, Kim SH, Lee JM, Kim SW, Jang JY, Han JK, et al. Preoperative assessment of resectability of hepatic hilar cholangiocarcinoma: combined CT and cholangiography with revised criteria. *Radiology* 2006;239:113-121
22. Franken LC, Coelen RJS, Erdmann JI, Verheij J, Kop MP, van Gulik TM, et al. Multidetector computed tomography assessment of vascular involvement in perihilar cholangiocarcinoma. *Quant Imaging Med Surg* 2021;11:4514-4521
23. Rassam F, Roos E, van Lienden KP, van Hooft JE, Klümpen HJ, van Tienhoven G, et al. Modern work-up and extended resection in perihilar cholangiocarcinoma: the AMC experience. *Langenbecks Arch Surg* 2018;403:289-307

 https://doi.org/10.3348/kjr.2023.0368